Input-to-state Stability on Formation Graphs

Herbert G. Tanner[1] George J. Pappas[2] Vijay Kumar [3]

Abstract

Formation stability is now analyzed under a new prism using input-to-state stability. Formation ISS relates leader input to internal state of the formation and characterizes the way this input affects stability performance. Compared to other notions of stability for interconnected systems, formation ISS does not require attenuation of errors as they propagate, but instead quantifies the amplification and provides worst case bounds. The control interconnections that give rise to the formation are represented by a graph. The formation graphs considered are built from a small number of primitive graphs, the stability properties of which are used to reason about the composite. For the case of linear dynamics, a recursive expression allows the calculation of the bounds using the graph theoretic representation of the formation via the adjacency matrix. Illustrative examples demonstrate how formation ISS can be used as an analysis and a design tool.

1 Introduction

Control and coordination of multi-agent systems has been an active area of research in the last years, motivated by recent advances in computation and communication and a large number of application areas such as automated highway systems [1, 2], cooperative robot reconnaissance [3] and manipulation [4, 5], formation flight control [6, 7] and satellite clustering [8] . Analysis methods for these kind of control interconnections between (possibly heterogeneous) systems, is therefore an important issue [9]. Existing methods are based mainly on three different approaches to interconnection architecture. In the behavior based approach [3] each agent is thought of being able to exhibit a number of primary behaviors. Another approach focuses on maintaining a certain group configuration and forces each agent to behave as a particle in a rigid virtual structure [10, 11]. The leader-follower approach [7, 12] distinguishes a designated leader which the other agents follow.

[1]GRASP Lab, 3401 Walnut Street, Suite 300C, University of Pennsylvania, Philadelphia, PA 19104-6228 , e-mail: tanner@grasp.cis.upenn.edu

[2]Department of Electrical and Systems Engineering, 200 South 33rd Street, University of Pennsylvania, Philadelphia, PA 19104, e-mail: pappasg@ee.upenn.edu

[3]GRASP Lab, 3401 Walnut Street, Suite 300C, University of Pennsylvania, Philadelphia, PA 19104-6228 , e-mail: kumar@grasp.cis.upenn.edu

Stability properties of interconnected systems has been investigated using string stability [13, 2]. In more dimensions, string stability has been generalized to mesh stability [14], which expresses the property of each interconnection to suppress disturbances as they propagate. In [14] it has been shown that exponential stability of each unforced system and global Lipschitz continuity are sufficient conditions for mesh stability.

The approach presented in this paper is motivated by the propagation properties of input-to-state stability [15]. We consider formations that are based on leader-following and define *formation input-to-state stability (ISS)*, that relates leader input to formation internal state. Preliminary work on formation ISS [16] suggests that this notion can be used to define a performance measure in leader-follower formations. While approaches based on string and mesh stability [2, 17] aim at suppressing error propagation, we allow errors to amplify focusing on quantifying and bounding the amplification. Since 'week interaction' conditions [2] are not imposed, we are able to analyze a much richer class of interconnected systems and local controllers. Formation ISS bounds can be used to derive leader motion specifications that guarantee the boundedness of formation errors and suggest ways of improving performance by changing interconnection topology.

The paper is organized as follows: in Section 2 the interconnection topology is defined using graph theoretic terminology and the notion of formation input-to-state stability is defined. Section 3 presents our results on ISS propagation the systems involved are described by nonlinear dynamic equations. Section 4 specializes in the linear case, where conditions for ISS and resulting gains turn out to be less conservative. In Section 5 combinatorial expressions for the ISS gains for the formation graph and its subgraphs are provided, in which the topology of the formation appears explicitly in the form of the adjacency matrix. Finally, examples illustrate the use of the notion of formation ISS in Section 6 and Section 7 summarizes the results of this work.

2 Formation Control Graphs

Previous work has motivated the use of graphs to represent agent interaction [6, 12, 18] In this paper, the control-related interconnections between the agents of a formation are being modeled by means of a (directed)

formation control graph. The vertices of the graph correspond to the agents in the formation and the edges represent leader-follower relationships.

Definition 2.1 (Formation Control Graph) *A formation control graph $F_c = (V, E, D)$ is a directed graph that consists of:*

- *A finite set $V = \{v_1, \ldots, v_p\}$ of vertices and a mapping that assigns to each vertex v_i a control system describing the dynamics of a particular agent: $\dot{x}_i = f_i(x_i, u_i)$, where $x_i \in \mathbb{R}^n$ is the state of the agent and $u_i \in \mathbb{R}^m$ is the control input.*
- *A binary relation $E \subset V \times V$ representing a leader-follower relationship between agents, such that $(v_j, v_i) \in E$, if u_i depends on x_j.*
- *A finite set of formation specifications D indexed by the set E, $D = \{d_{ij}\}$. For each edge (v_j, v_i), $d_{ij} \in \mathbb{R}^n$, denotes the desired relative state between agent i and agent j.*

The class of formation graphs considered in this paper are directed acyclic graphs. Vertices with no incoming edges, are formation leaders, $v_\ell \in L \subset V$. Every follower is responsible for meeting the specifications on the edges incoming to it. We assume that the formation specifications $\{d_{ij}\}$ are constant. In case of many incoming edges, the desired state for a follower j is formed as: $x_j^r = \sum_i S_{ij}(x_i - x_j - d_{ij})$, where S_{ij} are projection matrices such that $\sum_i \text{rank} S_{ij} = n$. Then the agent error is defined as the deviation from that desired state: $\tilde{x}_i \triangleq x_i^r - x_i$. The formation error $\tilde{x}$ is defined by stacking the errors of all the agents $v_i \in V$: $\tilde{x} \triangleq (\tilde{x}_1, \ldots, \tilde{x}_p)$. Our aim is to investigate the stability properties of the formation with respect to the input u_ℓ, of the formation leaders:

Definition 2.2 (Formation ISS) *A formation is called input-to-state stable if there is a class $\mathcal{KL}$ function β and a class $\mathcal{K}$ function γ such that for any initial formation error $\tilde{x}(0)$ and for any bounded inputs of the formation leaders $u_\ell(t)$, the formation error satisfies:*

$$\|\tilde{x}(t)\| \leq \beta(\|\tilde{x}(0)\|, t) + \textstyle\sum_{\ell \in L} \gamma(\sup_{[0,t]} \|u_\ell\|) \qquad (1)$$

We consider three primitive subgraphs of diameter two, which serve as building blocks: the cascade interconnection of three agents (Figure 1), the parallel interconnection of four agents (Figure 2) and the multiple-leader interconnection (Figure 3). These three primitive subgraphs, and graphs that can be decomposed into these subgraphs, are representative of a fairly broad class of formations.

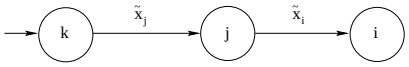


Figure 1: Cascade interconnection of agents.

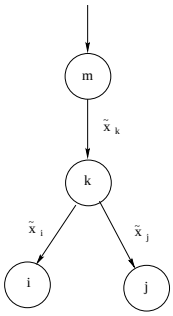


Figure 2: Parallel interconnection.

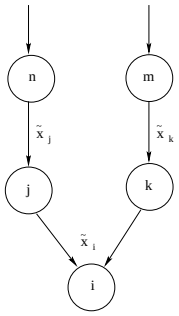


Figure 3: Multiple leader interconnection.

We prove the ISS property of the primitive subgraphs and we show how we can propagate the property when these primitives are connected. Exploiting the propagation properties of input-to-state stability we can derive a bound for the formation error that depends on the leaders input and the initial errors. Such a relationship is important, firstly because it allows to derive specifications for the leader behavior in order for stability of the group to be preserved and secondly can serve as a measure for comparison between different interconnection structures. One can then investigate the effect of interconnection changes on formation stability.

3 Formation ISS for Nonlinear Agents

Consider a leader-follower interconnection, such as the one depicted in Figure 1. Let the dynamics of the leader j and the follower i be given, respectively:

$$\begin{aligned} \dot{x}_j &= f_j(x_j, u_j) \\ \dot{x}_i &= f_i(x_i, u_i) \end{aligned} \qquad (2)$$

and let a feedback control law $u_i(x_i, x_j)$ be applied to the follower to meet the specifications d_{ji}. Follower error dynamics, $\tilde{x}_i = x_j - d_{ji} - x_i$ can be written as:

$$\dot{\tilde{x}}_i = \tilde{f}_i(x_i, x_j) + f_j(x_j, u_j) \qquad (3)$$

Lemma 3.1 *Let (2) be ISS with respect to u_j and (3) be ISS with respect to x_j and u_j:*

$$\|x_j(t)\| \leq \beta_j(\|x_j(0)\|, t) + \gamma_j(\sup \|u_j\|)$$
$$\|\tilde{x}_i(t)\| \leq \beta_i(\|\tilde{x}_i(0)\|, t) + \gamma_{i_1}(\sup \|u_j\|) + \gamma_{i_2}(\sup \|x_j\|)$$

for some $\mathcal{KL}$ functions β_j, β_i and some $\mathcal{K}$ functions γ_j, γ_{i_1} and γ_{i_2}. Then (2)-(3) is ISS.

Proof: Since γ_{i_1} and γ_{i_2} are class $\mathcal{K}$, $\gamma_{i_1}(\sup_{s\leq\tau\leq t}\|u_j\|) \leq \gamma_{i_1}(\sup_{s\leq\tau\leq t}\|u_j\| + \sup_{s\leq\tau\leq t}\|x_j\|)$ and $\gamma_{i_2}(\sup_{s\leq\tau\leq t}\|u_j\|) \leq \gamma_{i_2}(\sup_{s\leq\tau\leq t}\|u_j\| + \sup_{s\leq\tau\leq t}\|x_j\|)$. Then it is always possible to find a class $\mathcal{K}$ function γ_i such that $\gamma_i(\sup_{s\leq\tau\leq t}\|u_j\| + \sup_{s\leq\tau\leq t}\|x_j\|) \leq \gamma_{i_1}(\sup_{s\leq\tau\leq t}\|u_j\|+\sup_{s\leq\tau\leq t}\|x_j\|)+ \gamma_{i_2}(\sup_{s\leq\tau\leq t}\|u_j\| + \sup_{s\leq\tau\leq t}\|x_j\|)$. By application of known results on the cascading ISS systems ([19]-Appendix) the proof is completed. ■

Consider five agents i, j, k, m and n. First let agents i, j and k be connected in cascade (Figure 1), where i is assigned to follow j, j should follow k and k may have to follow some reference trajectory $y(t)$. Define the errors for agents i, j and k as:

$$\tilde{x}_i \triangleq x_i^r - x_i \equiv x_j - d_{ij} - x_i$$
$$\tilde{x}_j \triangleq x_j^r - x_j \equiv x_k - d_{jk} - x_j$$
$$\tilde{x}_k \triangleq x_k^r - x_k \equiv x_m - d_{km} - x_k$$

Suppose that control laws $u_i = u_i(x_i, x_j)$, $u_j = u_j(x_j, x_k)$ and $u_k = u_k(x_k, x_m)$ are designed so that each follower can track its leader, and the closed loop error dynamics can take the form:

$$\dot{\tilde{x}}_i = \tilde{f}_i(t, \tilde{x}_i, \tilde{x}_j) \quad (4)$$
$$\dot{\tilde{x}}_j = \tilde{f}_j(t, \tilde{x}_j, \tilde{x}_k) \quad (5)$$
$$\dot{x}_k = f_k(t, \tilde{x}_k) \quad (6)$$

Proposition 3.2 (Nonlinear Cascade) *If* (4) *and* (5) *are ISS with respect to $\tilde{x}_j$ and $\tilde{x}_k$ respectively, then the $\tilde{x}_g = (\tilde{x}_i, \tilde{x}_j)$-system is ISS with respect to $\tilde{x}_k$:*

$$\|\tilde{x}_g(t)\| \leq \beta_g(\|\tilde{x}_g(0)\|, t) + \gamma_{g_k}(\sup\|\tilde{x}_k\|)$$

where

$$\beta_g(r,t) = \beta_i(2\beta_i(r, t/2) + 2\gamma_{i_j}(2\beta_j(r,0)), t/2) + \gamma_{i_j}(2\beta_j(r, t/2)) + \beta_j(r,t),$$
$$\gamma_{g_k}(r) = \beta_i(2\gamma_{i_j}(2\gamma_{j_k}(r)), 0) + \gamma_{i_j}(2\gamma_{j_k}(r)) + \gamma_{j_k}(r).$$

Proof: Follows from Lemma 3.1 and the ISS pair expressions derived for cascading ([19]-Appendix). ■

Consider the parallel interconnection of Figure 2. Agents i and j are assigned to follow agent k, and k follows the group leader m. Application of the feedback laws $u_i = u_i(x_i, x_k)$, $u_j = u_j(x_j, x_k)$, $u_k = u_k(x_k, x_m)$ can bring the closed loop error dynamics to the form:

$$\dot{\tilde{x}}_i = \tilde{f}_i(t, \tilde{x}_i, \tilde{x}_k) \quad (7)$$
$$\dot{\tilde{x}}_j = \tilde{f}_j(t, \tilde{x}_j, \tilde{x}_k) \quad (8)$$
$$\dot{\tilde{x}}_k = \tilde{f}_k(t, \tilde{x}_k, \tilde{x}_m) \quad (9)$$

where $\tilde{x}_i = x_k - d_{ki} - x_i$, $\tilde{x}_j = x_k - d_{kj} - x_j$ and $\tilde{x}_k = x_m - d_{mk} - x_k$.

Proposition 3.3 (Nonlinear Parallel) *Let* (7) *with input $\tilde{x}_k$ and* (8) *with input $\tilde{x}_k$ be ISS and* (9) *be ISS with respect to $\tilde{x}_m$:*

$$\|\tilde{x}_i(t)\| \leq \beta_i(\|x_i(0)\|, t) + \gamma_{i_k}(\sup\|\tilde{x}_k\|) \quad (10)$$
$$\|\tilde{x}_j(t)\| \leq \beta_j(\|x_j(0)\|, t) + \gamma_{j_k}(\sup\|\tilde{x}_k\|) \quad (11)$$
$$\|\tilde{x}_m(t)\| \leq \beta_m(\|x_m(0)\|, t) + \gamma_{k_m}(\sup\|\tilde{x}_m\|) \quad (12)$$

Then the composed $\tilde{x}_g = (\tilde{x}_i, \tilde{x}_j, \tilde{x}_k)$-system is ISS with respect to $\tilde{x}_m$ with gain functions:

$$\beta_g(r,s) = \beta_i(2\beta_i(r, s/2) + 2\gamma_{i_k}(2\beta_k(r,0)), s) + \gamma_{i_k}(2\beta_k(r, s/2)) + \beta_j(2\beta_j(r, s/2) + 2\gamma_{j_k}(2\beta_k(r,0)), s) + \gamma_{j_k}(2\beta_k(r, s/2)) + \beta_k(r,s)$$
$$\gamma_{g_k}(r) = \beta_i(2\gamma_{i_k}(2\gamma_{k_m}(r)), 0) + \gamma_{i_k}(2\gamma_{k_m}(r)) + \beta_j(2\gamma_{j_k}(2\gamma_{k_m}(r)), 0) + \gamma_{j_k}(2\gamma_{k_m}(r)) + \gamma_{k_m}(r)$$

Proof: From (10) and (11) for interval $[t/2, t]$:

$$\|\tilde{x}_i(t)\| \leq \beta_i(\|\tilde{x}_i(t/2)\|, t) + \gamma_{i_k}(\sup_{[t/2,t]}\|\tilde{x}_k\|),$$
$$\|\tilde{x}_j(t)\| \leq \beta_j(\|\tilde{x}_j(t/2)\|, t) + \gamma_{j_k}(\sup_{[t/2,t]}\|\tilde{x}_k\|)$$

For the interval $[0, t/2]$ the same relations yield:

$$\|\tilde{x}_i(t/2)\| \leq \beta_i(\|\tilde{x}_i(0)\|, t/2) + \gamma_{i_k}(\sup_{[0,t/2]}\|\tilde{x}_k\|),$$
$$\|\tilde{x}_j(t/2)\| \leq \beta_j(\|\tilde{x}_j(0)\|, t/2) + \gamma_{j_k}(\sup_{[0,t/2]}\|\tilde{x}_k\|)$$

From ISS of the $\tilde{x}_k$ subsystem we obtain:

$$\sup_{[0,t/2]}\|\tilde{x}_k\| \leq \beta_k(\|\tilde{x}_k(0)\|, 0) + \gamma_{k_m}(\sup\|\tilde{x}_m\|),$$
$$\sup_{[t/2,t]}\|\tilde{x}_k\| \leq \beta_k(\|\tilde{x}_k(0)\|, t/2) + \gamma_{k_m}(\sup\|\tilde{x}_m\|)$$

Substituting and combining with (12) we obtain for the $\tilde{x}_g = (\tilde{x}_i, \tilde{x}_j, \tilde{x}_k)$ system:

$$\|\tilde{x}_g\| \leq \Big\{\beta_i(2\beta_i(\|\tilde{x}_g(0)\|, t/2) + 2\gamma_{i_k}(2\beta_k(\|\tilde{x}_g(0)\|, 0)), t) + \gamma_{i_k}(2\beta_k(\|\tilde{x}_g(0)\|, t/2)) + \beta_j(2\beta_j(\|\tilde{x}_g(0)\|, t/2) + 2\gamma_{j_k}(2\beta_k(\|\tilde{x}_g(0)\|, 0)), t) + \gamma_{j_k}(2\beta_k(\|\tilde{x}_g(0)\|, t/2)) + \beta_k(\|\tilde{x}_g(0)\|, t)\Big\} + \Big\{\beta_i(2\gamma_{i_k}(2\gamma_{k_m}(\sup\|\tilde{x}_m\|)), 0) + \gamma_{i_k}(2\gamma_{k_m}(\sup\|\tilde{x}_k\|)) + \beta_j(2\gamma_{j_k}(2\gamma_{k_m}(\sup\|\tilde{x}_m\|)), 0) + \gamma_{j_k}(2\gamma_{k_m}(\sup\|\tilde{x}_k\|)) + \gamma_{k_m}(\sup\|\tilde{x}_m\|)\Big\}$$

■

The multiple leader interconnection of Figure 3 is realized by the feedback control laws $u_i = u_i(x_i, x_j, x_k)$, $u_j = u_j(x_j, x_n)$, $u_k = u_k(x_k, x_m)$ that can bring the closed loop error dynamics to the following form:

$$\dot{\tilde{x}}_i = \tilde{f}_i(t, \tilde{x}_i, \tilde{x}_j, \tilde{x}_k) \quad (13)$$
$$\dot{\tilde{x}}_j = \tilde{f}_j(t, \tilde{x}_j, \tilde{x}_n) \quad (14)$$
$$\dot{\tilde{x}}_k = \tilde{f}_k(t, \tilde{x}_k, \tilde{x}_m) \quad (15)$$

Proposition 3.4 (Nonlinear Multiple-Leader) *Let* (13) *be ISS with respect to* $\tilde{x}_j$ *and* $\tilde{x}_k$, (14) *be ISS with respect to* $\tilde{x}_n$ *and* (15) *be ISS with respect to* $\tilde{x}_m$*:*

$$\|\tilde{x}_i(t)\| = \beta_i(\|\tilde{x}_i(0)\|, t) + \gamma_{i_j}(\sup\|\tilde{x}_j\|) + \gamma_{i_k}(\sup\|\tilde{x}_k\|) \quad (16)$$

$$\|\tilde{x}_j(t)\| = \beta_j(\|\tilde{x}_j(0)\|, t) + \gamma_{j_n}(\sup\|\tilde{x}_n\|) \quad (17)$$

$$\|\tilde{x}_k(t)\| = \beta_k(\|\tilde{x}_k(0)\|, t) + \gamma_{k_m}(\sup\|\tilde{x}_m\|) \quad (18)$$

Then the composed $\tilde{x}_g = (\tilde{x}_i, \tilde{x}_j, \tilde{x}_k)$*-system is ISS with respect to* $\tilde{x}_n$ *and* $\tilde{x}_m$*:*

$$\|\tilde{x}_g(t)\| \leq \beta_g(\|\tilde{x}_g(0)\|, t) + \gamma_{g_n}(\sup\|\tilde{x}_n\|) + \gamma_{g_m}(\sup\|\tilde{x}_m\|)$$

where

$$\beta_g(r,s) = \beta_i(2\beta_i(r,\tfrac{s}{2}) + 2\gamma_{i_j}(2\beta_j(r,0)) + 2\gamma_{i_k}(2\beta_k(r,0)), \tfrac{s}{2}) + \gamma_{i_j}(2\beta_j(r,\tfrac{s}{2})) + \gamma_{i_k}(2\beta_k(r,\tfrac{s}{2})) + \beta_j(r,s) + \beta_k(r,s)$$
$$\gamma_{g_n}(r) = \beta_i(4\gamma_{i_j}(2\gamma_{j_n}(r)),0) + \gamma_{i_j}(2\gamma_{i_n}(r)) + \gamma_{j_n}(r),$$
$$\gamma_{g_m}(r) = \beta_i(4\gamma_{i_k}(2\gamma_{k_m}(r)),0) + \gamma_{i_k}(2\gamma_{k_m}(r)) + \gamma_{k_m}(r)$$

Proof: From (16): $\|\tilde{x}_i(t/2)\| \leq \beta_i(\|\tilde{x}_i(0)\|, t/2) + \gamma_{i_j}(\sup_{[0,\frac{t}{2}]}\|\tilde{x}_j\|) + \gamma_{i_k}(\sup_{[0,\frac{t}{2}]}\|\tilde{x}_k\|)$. Setting initial time to $\frac{t}{2}$: $\|\tilde{x}_i(t)\| \leq \beta_i(\|\tilde{x}_i(t/2)\|, t) + \gamma_{i_j}(\sup_{[\frac{t}{2},t]}\|\tilde{x}_j\|) + \gamma_{i_k}(\sup_{[\frac{t}{2},t]}\|\tilde{x}_k\|)$. Substituting for $\|\tilde{x}_i(t/2)\|$, and for $\|\tilde{x}_j\|$, $\|\tilde{x}_k\|$ from (17), (18), respectively, and adding (17) - (18) the result follows. ■

4 The Linear Case

Linearity allows for less conservative bounds than those obtainable from Propositions 3.2, 3.3 and 3.4, primarily because of the ability to exactly decompose the $\mathcal{K}$ class functions. The computation of ISS gain functions β, γ can be performed using a recursive formula. The proofs of the statements for the linear case, similar in spirit with that of Proposition 3.3, will be omitted due to lack of space.

Consider the cascade interconnection of Figure 1 and suppose that the dynamics of agents i and j can be described by linear differential equations, where the pairs (A_i, B_i) and (A_j, B_j) are controllable:

$$\dot{x}_i = A_i x_i + B_i u_i, \quad \dot{x}_j = A_j x_j + B_j u_j \quad (19)$$

For $x_i^r = x_j - d_{ij}$ to be an equilibrium of the closed loop control system: $\dot{x}_i = A_i x_i + B_i u_i$, it should hold that $A_i x_i^r \in \mathcal{R}(B_i)$. Suppose there exists e_{ij} such that $B_i e_i = -A_i x_i^r$. Application of the following control law for the follower: $u_i = K_i(x_j - x_i - d_{ij}) + e_{ij}$ and using standard linear systems theory:

$$\|\tilde{x}_i(t)\| \leq \hat{\beta}_i \|\tilde{x}_i(0)\| \, \mathrm{e}^{-\frac{1-\theta}{2\lambda_M[P_i]}t} + \hat{\gamma}_{i_j} \sup(\|\dot{x}_j\|) \quad (20)$$

where $\hat{\beta}_i = \left(\frac{\lambda_M[P_i]}{\lambda_m[P_i]}\right)^{\frac{1}{2}}$, $\hat{\gamma}_{i_j} = \frac{2(\lambda_M[P_i])^{\frac{3}{2}}}{(\lambda_m[P_i])^{\frac{1}{2}}\theta}$. and P_i is the solution of the Lyapunov equation $P_i(A_i - B_i K_i) + (A_i - B_i K_i)^T P_i = -I$, and $\theta \in (0,1)$. Equation (20) implies that the closed loop system is input-to-state stable with respect to $\dot{x}_j$ as input and gain functions: $\beta_i(r,t) = r\hat{\beta}_i \mathrm{e}^{-\frac{1-\theta}{2\lambda_M[P_i]}t}$, $\gamma_{i_j}(r) = \hat{\gamma}_{i_j} r$. Apply the following linear feedback:

$$u_i = K_i\tilde{x}_i + e_i, \; u_j = K_j\tilde{x}_j + e_j, \; u_k = K_k\tilde{x}_k + e_k \quad (21)$$

where e_i, e_j and e_k are such that: $B_i e_i = -A_i x_i^r$, $B_j e_j = -A_j x_j^r$, and $B_k e_k = -A_k x_k^r$.

Corollary 4.1 (Linear Cascade) *Consider the interconnection of Figure 1 where agents have linear dynamics of the form* (19)*. Then the application of control laws* (21) *results in a closed loop* $\tilde{x}_g = (\tilde{x}_i, \tilde{x}_j)$*-system which is ISS with respect to* $\tilde{x}_k$*:*

$$\|\tilde{x}_g(t)\| \leq \bar{\beta}_g \|\tilde{x}_g(0)\| \, e^{-\mu t} + \bar{\gamma}_{g_k} \sup\|\tilde{x}_k\|$$

where $\mu \triangleq \frac{1-\theta}{4\max\{\lambda_M[P_i], \lambda_M[P_j]\}}$ *and*

$$\bar{\beta}_g \triangleq \bar{\beta}_i^2 + ((\bar{\beta}_j + \bar{\beta}_i)\bar{\gamma}_{i_j} + 1)\bar{\beta}_j,$$
$$\bar{\gamma}_{g_k} \triangleq ((\bar{\beta}_i + \bar{\beta}_j + 1)\bar{\gamma}_{i_j} + 1)\bar{\gamma}_{j_k}$$

where

$$\bar{\beta}_i = \left(\frac{\lambda_M[P_i]}{\lambda_m[P_i]}\right)^{\frac{1}{2}}, \; \bar{\gamma}_{i_j} = \frac{2(\lambda_M[P_i])^{\frac{3}{2}}\lambda_M[A_j - B_j K_j]}{(\lambda_m[P_i])^{\frac{1}{2}}\theta} \quad (22)$$

For the parallel interconnection of Figure 2 it can also be shown that the application of appropriate feedback laws can renter the closed loop system ISS with respect to the error of the group leader:

Corollary 4.2 (Linear Parallel) *Consider the parallel interconnection of Figure 2 where the agents have dynamics of the form* (19)*. Then the application of linear feedback* $u_r = K_r\tilde{x}_r + e_r$, $r = \{i, j, k, m\}$*, results in a closed loop system for* $\tilde{x}_g = (\tilde{x}_i, \tilde{x}_j, \tilde{x}_k)$ *which is ISS with respect to* $\tilde{x}_m$*:*

$$\|\tilde{x}_g\| \leq \bar{\beta}_g \|\tilde{x}_g(0)\| \, e^{-\mu t} + \bar{\gamma}_{g_m} \sup\|\tilde{x}_m\|$$

where $\mu = \frac{1-\theta}{4\max\{\lambda_M[P_i], \lambda_M[P_j], \lambda_M[P_k]\}}$,

$$\bar{\beta}_g = \bar{\beta}_i^2 + \bar{\beta}_j^2 + ((\bar{\beta}_k + \bar{\beta}_i)\bar{\gamma}_{i_k} + (\bar{\beta}_k + \bar{\beta}_j)\bar{\gamma}_{j_k} + 1)\bar{\beta}_k,$$
$$\bar{\gamma}_{g_k} = ((\bar{\beta}_i + \bar{\beta}_k + 1)\bar{\gamma}_{i_k} + (\bar{\beta}_j + \bar{\beta}_k + 1)\bar{\gamma}_{j_k} + 1)\bar{\gamma}_{k_m},$$

and $\bar{\beta}_i$, $\bar{\gamma}_{i_j}$ *given by* (22)*.*

In the interconnection of multiple leaders depicted in Figure 3 the linear feedback will be of the form:

$$u_i = e_i + K_i\tilde{x}_i \qquad u_j = e_j + K_j\tilde{x}_j \qquad u_k = e_k + K_k\tilde{x}_k$$
$$u_m = e_m + K_m\tilde{x}_m \qquad u_n = e_n + K_n\tilde{x}_n \quad (23)$$

where e_i, e_j and e_k satisfy $B_i e_i = -A_i x_i^r$, $B_j e_j = -A_j x_j^r$, $B_k e_k = -A_k x_k^r$, $B_m e_m = -A_m x_m^r$ and $B_n e_n = -A_n x_n^r$. and K_s, $s \in \{i, j, k, m, n\}$, selected to make $(A_s - B_s K_s)$, Hurwitz.

Corollary 4.3 (Linear Multiple-Leader) *Consider the interconnection of Figure 3 where agents i, j, k, n and m have dynamics of the form* (19). *Then control laws* (23) *result in a closed loop system for $\tilde{x}_g = (\tilde{x}_i, \tilde{x}_j, \tilde{x}_k)$ which is ISS with respect to $\tilde{x}_m$ and $\tilde{x}_n$:*

$$\|\tilde{x}_g\| \leq \bar{\beta}_g \|\tilde{x}_g(0)\| e^{-\mu t} + \bar{\gamma}_{g_n} \sup \|\tilde{x}_n\| + \bar{\gamma}_{g_m} \sup \|\tilde{x}_m\|$$

where $\mu = \frac{1-\theta}{4 \max\{\lambda_M[P_i], \lambda_M[P_j], \lambda_M[P_k]\}}$, $\bar{\gamma}_{i_k}$ *as in* (22),

$$\bar{\beta}_g = \bar{\beta}_i^2 + (\bar{\beta}_j + \bar{\beta}_i)\bar{\beta}_j\bar{\gamma}_{i_j} + (\bar{\beta}_k + \bar{\beta}_i)\bar{\beta}_k\bar{\gamma}_{i_k}) + \bar{\beta}_j + \bar{\beta}_k$$
$$\bar{\gamma}_{g_n} = (\bar{\gamma}_{i_j}(1 + \bar{\beta}_j + \bar{\beta}_i) + 1)\bar{\gamma}_{j_n},$$
$$\bar{\gamma}_{g_m} = (\bar{\gamma}_{i_k}(\bar{\beta}_k + \bar{\beta}_i) + 1)\bar{\gamma}_{k_m}$$

5 The Adjacency Matrix in Formation ISS

The ISS gain expressions of Corollaries 4.1, 4.2, 4.3 can be grouped into a single formula that enables abstracting a primitive graph of diameter two into a diameter one, equivalent from the stability point of view. Used recursively, they provide a computational means of deriving the formation ISS gains. Consider the adjacency matrix of the formation graph, A and define constant matrices Γ, B as follows:

$$B = [b_{ij}], \text{ where } \begin{cases} b_{ij} = \bar{\beta}_j, \text{ if } i = j \\ b_{ij} = 0, \text{otherwise} \end{cases}$$

$$\Gamma = [g_{ij}], \text{ where } \begin{cases} g_{ij} = \bar{\gamma}_{j_i}, \text{ if } (v_i, v_j) \in E \\ g_{ij} = 0, \text{otherwise} \end{cases}$$

It can be shown by direct calculation that the matrices:

$$B_1 = B + (AB^2 + B^2\Gamma + B\Gamma B)A^T \quad (24a)$$
$$\Gamma_1 = \Gamma + (\Gamma^2(I + B) + \Gamma B\Gamma)A^T \quad (24b)$$

give the group ISS gains, for each primitive subgraph, with the (i, j) element corresponding to the particular group gain of the (i, j) interconnection. To provide a little insight to (24) observe the ISS gain expressions of Corollary 4.1: $\bar{\beta}_g = \bar{\beta}_i^2 + \bar{\beta}_j^2\bar{\gamma}_{i_j} + \bar{\beta}_i\bar{\beta}_j\bar{\gamma}_{i_j} + \bar{\beta}_j$. It is easy to show that the first term in the above expession is provided by AB^2A^T, the second term by $B^2\Gamma A^T$, the third by $B\Gamma BA^T$ and the last by B. The same reasoning can be applied for Γ_1. The propagation is performed through matrix products of the form A^2A^T in the expression for Γ_1 which can be shown to provide the number of paths of length two starting with a specified edge. Propagation for B_1 is done through products of the form AA^T which give the number of immediate successors of a vertex. A detailed proof will be omitted here due to lack of space and will provided in a forthcoming publication.

Due to linearity, combinations of the three primitive graphs can be superimposed, and therefore, equations (24) can be used to abstract any formation graph of diameter three into one of two. The ISS gains for the whole formation graph can then be computed using the recursive formulas, with $k = 1, \ldots, p$:

$$B_k = B + (AB_{k-1}^2 + B(B\Gamma_{k-1} + \Gamma_{k-1}B_{k-1})A^T \quad (25)$$
$$\Gamma_k = \Gamma + \Gamma(\Gamma(I + B_{k-1}) + B\Gamma)A^T, \quad (26)$$

In matrix B_p the element at position (i, j) denotes the linear gain of the transient term bounding the errors in the part of the formation where agent j is the group leader following agent i. Similarly, an entry at position (i, j) in Γ_p matrix, gives the gain of input from agent i to the error of the group where agent j is the leader.

6 Examples

Equations (25)-(26) provide a computational way of assessing the performance of leader-follower formations in terms of stability. Intuitively, it may be clear that the interconnection of Figure 2 can outperform that of Figure 1 because of error propagation. This can now be formally shown using (26). Assume identical dynamics and control laws for all agents so that for all $s \in \{i, j, k, m\}$, $\bar{\beta}_s = 1.2$ and $\bar{\gamma}_s = 1.8$, (due to identical dynamics, the leader of each agent is insignificant). Then it turns out that the input gain is significantly increased in the cascade case $\bar{\gamma}^{cas} = 34.2778$ than in the parallel case $\bar{\gamma}^{par} = 23.832$. Note however the dependence of the comparison result on the dynamics: if the gains are sufficiently small, e.g. with $\bar{\gamma}_s = 0.8$ and $\bar{\beta}_s = 0.2$, the error reaching agent i in the cascade interconnection will have attenuate and will be smaller than the corresponding error propagated in the parallel formation. In this case ISS gain calculation yields: $\bar{\gamma}^{cas} = 1.76256$ and $\bar{\gamma}^{par} = 2.592$.

Equations (25)-(26) can also help to draw conclusions about ways to improve performance. Consider the formation of Figure 4. For a given a range of values for the leader input, the estimated region for the formation errors could be unacceptably large. If however, the input gain for the group $(2, 3, 5, 6)$, $\gamma_F^1 = \bar{\gamma}_{3_2}(1 + (1 + \bar{\beta}_3 + \bar{\beta}_5)\bar{\gamma}_{5_3} + (1 + \bar{\beta}_3 + \bar{\beta}_6)\bar{\gamma}_{6_3})$, is small enough, one could consider breaking the formation by eliminating the edge $(2, 3)$ if the gain of the remaining part, $\gamma_F^2 = \bar{\gamma}_{2_1}(1 + (1 + \bar{\beta}_2 + \bar{\beta}_4)\bar{\gamma}_{4_2})$ is small enough.

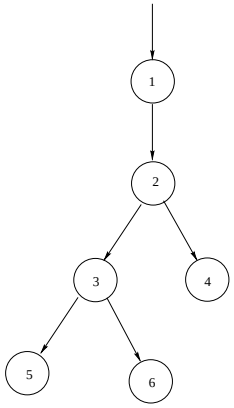


Figure 4: Example formation.

7 Conclusion

Formation input-to-state stability is a new notion of stability for interconnected systems that can be used in the performance analysis and design of formations. It yields quantitative measures of the performance of leader-follower formation structures in terms of stability. The class of formation structures considered can be described by connected, acyclic directed graphs, which can be constructed by combination and superposition of primitive types of subgraphs. It is shown how ISS can be propagated through the formation graph and how performance measures can be calculated. Illustrative examples show how formation ISS can be used to perform stability analysis and guide control design.

Acknowledgments: This research is partially supported by DARPA MICA Contract Number N66001-01-C-8076, and by DARPA/AFRL Software-Enabled Control Grant F33615-01-C-1848.

References

[1] P. Varaiya, "Smart cars on smart roads: problems of control," *IEEE Transactions on Automatic Control*, vol. 38, no. 2, pp. 195–207, 1993.

[2] D. Swaroop and J. K. Hedrick, "Sting stability of interconnected systems," *IEEE Transactions on Automatic Control*, vol. 41, pp. 349–357, March 1996.

[3] T. Balch and R. Arkin, "Behavior-based formation control for multirobot systems," *IEEE Transactions on Robotics and Automation*, vol. 14, no. 12, 1998.

[4] H. Tanner and K. Kyriakopoulos, "Nonholonomic motion planning for mobile manipulators," in *Proc. of the 2000 IEEE International Conference on Robotics and Automation*, (San Francisco), pp. 1233–1238, April 2000.

[5] T. Sugar, J. Desai, V. Kumar, and J. P. Ostrowski, "Coordination of multiple mobile manipulators," in *Proceedings of IEEE International Conference on Robotics Automation*, vol. 3, pp. 3022–2027, 2001.

[6] M. Mesbahi and F. Hadaegh, "Formation flying of multiple spacecraft via graphs, matrix inequalities, and switching," *AIAA Journal of Guidance, Control and Dynamics*, vol. 24, pp. 369–377, March 2001.

[7] R. W. Beard, J. Lawton, and F. Y. Hadaegh, "A coordination architecture for spacecraft formation control," *IEEE Transactions on Control Systems Technology*, vol. 9, pp. 777–790, November 2001.

[8] C. R. McInnes, "Autonomous ring formation for a planar constellation of satellites," *AIAA Journal of Guidance Control and Dynamics*, vol. 18, no. 5, pp. 1215–1217, 1995.

[9] D. Šiljak, *Large Scale Dynamic Systems: Stability and Structure*. North-Holland, 1978.

[10] K.-H. Tan and M. A. Lewis, "Virtual structures for high-precision cooperative mobile robot control," *Autonomous Robots*, vol. 4, pp. 387–403, October 1997.

[11] M. Egerstedt and X. Hu, "Formation constrained multi-agent control," in *Proceedings of the IEEE Conference on Robotics and Automation*, (Seoul, Korea), pp. 3961–3966, May 2001.

[12] P. Tabuada, G. J. Pappas, and P. Lima, "Feasible formations of multi-agent systems," in *Proceedings of the American Control Conference*, (Arlington, VA), pp. 56–61, June 2001.

[13] K. C. Chu, "Decentralized control of high speed vehicle strings," *Transportation Science*, vol. 8, pp. 361–383, 1974.

[14] A. Pant, P. Seiler, and K. Hedrick, "Mesh stability of look-ahead interconnected systems," *IEEE Transactions on Automatic Control*, vol. 47, pp. 403–407, Feb. 2002.

[15] E. D. Sontag and Y. Wang, "On characterizations of the input-to-state stability property," *Systems & Control Letters*, no. 24, pp. 351–359, 1995.

[16] H. G. Tanner, V. Kumar, and G. J. Pappas, "The effect of feedback and feedforward on formation ISS," in *IEEE International Conference on Robotics and Automation*, (Washington, DC.), pp. 3448–3453, 2002.

[17] D. Yanakiev and I. Kanellakopoulos, "A simplified framework for string stability analysis in AHS," in *Proceedings of the 13th IFAC World Congress*, (San Francisco, CA), pp. 177–182, July 1996.

[18] J. P. Desai, J. P. Ostrowski, and V. Kumar, "Modeling and control of formations of nonholonomic mobile robots," *IEEE Transactions on Robotics and Automation*, vol. 17, no. 6, pp. 905–908, 2001.

[19] M. Krstić, I. Kanellakopoulos, and P. Kokotović, *Nonlinear and Adaptive Control Design*. John Willey and Sons, 1995.